Chapter 7

Effect of promoter doping on catalytic activity of Cu_1Mn_8 catalyst for CO oxidation

7. General

The Cu_1Mn_8 catalyst is highly active for CO oxidation could be ascribed to the resonance system $Cu^{2+} + Mn^{3+} \leftrightarrows Cu^{+} + Mn^{4+}$ and the high adsorption of CO onto Cu^{2+}/Mn^{4+} and of O_2 onto Cu^{+}/Mn^{3+} [Peng *et al.,* 2011]. The Cu-oxide is found weakly active for CO oxidation, but in combination with Mn-oxide in appropriate proportions, some very active catalyst system is generated [Lee *et al.,* 2016]. Enhancement in the activity of Cu_1Mn_8 catalysts for CO oxidation has been attempted by combining copper, manganese with other elements like Ag, Au, Co, Ce and Fe etc. An addition of low level of these promoters into the Cu_1Mn_8 catalyst, yet this is an approach that has proven beneficial in other oxidation catalysts [Taylor *et al.,* 1999; Zhang *et al.,* 2016]. The addition of small amounts of (3wt.%) cobalt, cerium, iron and silver by deposition precipitation method, to a mixed Cu_1Mn_8 catalyst to improved their performance for CO oxidation and reduced their deactivation.

The Co_3O_4, a unique spinel-structure transition metal oxide finds numerous applications because of its outstanding properties in various fields. Co_3O_4 is the most active catalyst amongst the transition metal oxides for CO oxidation and shows the extraordinary activity and stability far below their ambient temperature under dry conditions [Ma 2014]. It has a mixed valence oxide couples Co^{3+}/Co^{2+} with Co^{3+} cations occupy 16 octahedral sites and Co^{2+} cations occupy 8 tetrahedral sites and 32 sites are occupied by O^{2-} ions. The Co^{3+} is regarded as the active site for CO oxidation, whereas the Co^{2+} is almost inactive in this reaction [Xie *et al.,* 2009]. CO oxidation is a structure-sensitive

reaction, i.e. exposer of different crystal planes of Co_3O_4 spinel shows diverse performance in CO oxidation [Skoglundh *et al.,* 1996]. The Co_3O_4 nano-rods shows much higher activity and better durability due to exposer of {110} planes rich in Co^{3+} sites than conventional Co_3O_4 nanoparticles having exposer of less active {001} and {111} planes containing inactive Co^{2+} sites [Samiee *et al.,* 2007]. The addition of Co into the Cu_1Mn_8 catalyst leads to enhance in the surface area and also increases the number of active sites present on the catalyst surface. Therefore, it has to shows the best performance for CO oxidation [Saeed *et al.,* 2012].

Silver oxide (AgO, Ag_2O, Ag_2O_3) based catalyst is measured as an attractive alternative to the other metal oxide catalysts because of its high availability, stability and activity for CO oxidation [Zhang *et al.,* 2010]. The performance of silver oxide based catalysts strongly depends upon their surface structure and their composition. It is depend upon the preparation method, reaction conditions and the size of silver nanoparticles [Kondrat *et al.,* 2011]. Activation of silver oxide based catalysts is often regarded as a result of the occurrence of various Ag–O interactions. The surface and subsurface oxygen atoms are reported to be the active sites for Ag based catalysts in many oxidation reactions [Cao *et al.,* 2017]. The role of different silver species has also been studied, and Ag^0 as an active species found to improve the catalytic activity at a low temperature [Chen *et al.,* 2013]. The highly dispersed Ag nanoparticles deposited on CuMnOx catalyst surfaces by the incipient wetness method. The CuMnOx supported silver oxides catalysts are very active for many deep oxidation reactions [Narasimharao *et al.,* 2015]. The catalytic activity of Ag promoted CuMnOx catalyst is highly influence by the addition of Ag to the molar ratio of Cu/Mn in CuMnOx catalyst [Hasegawa *et al.,* 2009].

Ceria has a high oxygen storage capability and high redox properties; therefore, it is making more oxygen accessible for the oxidation process [Skaf *et al.,* 2014].The copper oxide and supported copper oxides are identified to be highly active for CO oxidation [Liu and Flytzani-Stephanopoulos 1995]. In the majority of study, find out that the support CeO_2 plays a crucial role in Cu–CeO_2 catalyst for the total oxidation of CO, exhibiting a particular activity of various orders of magnitude superior to the conventional Cu-based catalysts and even comparable to precious metals [Kundakovic and Stephanopoulos 1998]. The addition of ceria into CuMnOx catalyst has also increased their activity and stability due to the increasing of meso/macro-pore volume and surface area after aging treatment. Compared with rare earth metals, the transition metals usually exhibit numerous oxidation states and better redox properties [Rodriguez *et al.,* 2017]. Good redox properties and strong interaction between the transition metals and ceria make the transition metal–Ce mixed oxides as candidate catalysts for CO oxidation [Guo *et al.,* 2016]. When ceria is doped into transition metal oxides, *in situ* forming cerium oxide could promote oxygen storage and release, enhance oxygen mobility and redox property of the catalyst [Zhang *et al.,* 2010].

As one of the important functional materials, the iron oxide (FeOx) has been broadly investigated in heterogeneous catalyst for its potential applications in CO oxidation. In general the FeOx supports include two different types: hydrated (Fe-OH), such as goethite or lepidocrocite FeOOH, and dehydrated (Fe-O), such as hematite α-Fe_2O_3, maghemite γ-Fe_2O_3 or magnetite Fe_3O_4 [Huang *et al.,* 2009]. Furthermore, the precipitation conditions of Fe^{2+} or Fe^{3+} precursor has been recognized as one of the key factors prevailing the structure and texture of the FeOx products [Sugimoto and Sakata 1992]. The objective of this study to understand the effect of different doped materials on the surface of Cu_1Mn_8 catalyst to improved their performance for CO oxidation. All

the catalysts are prepared in different calcination conditions like stagnant air, flowing air and reactive calcinations of (4.5% CO in air). This chapter described the intermediate compositions exhibiting the improved catalytic activity than the end composition, which was evidence of the synergism. The Cu_1Mn_8 was the most active reduced catalyst and the liability of lattice oxygen was one of the main factors that influence their activity. Activity of the doped Cu_1Mn_8 catalyst towards CO oxidation represents as the average oxidation number of Cu and Mn and the position nature of the different doped cations.

7.1 Experimental

7.1.1 Catalyst preparation

The Cu_1Mn_8 catalyst was prepared by the co-precipitation method, as discussed earlier in the Chapter 4. The different promoters like cobalt, cerium, silver and iron were doped (3wt.%) individually into the wet precursor of the prepared Cu_1Mn_8 catalyst. The nitrates of different promoters were used in doping followed by drying and calcination under different conditions such as stagnant air (SAC), flowing air (FAC) and reactive calcination (RC).

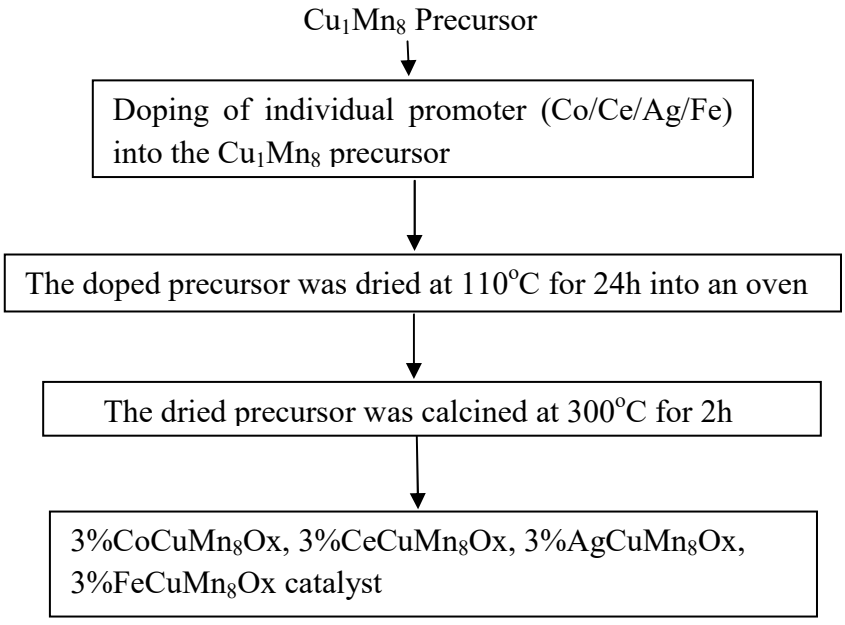

Figure 7.1: Preparation of (Co, Ce, Fe, Ag) doped Cu_1Mn_8 Catalyst

The RC was done in a reactive gas mixture consisting of 4.5% CO in air. The doping procedure is depicted in Figure 7.1. The nomenclature of the resulting catalysts thus obtained was given in Table 7.1.

Table 7.1: Nomenclature of prepared doped catalysts

Catalyst Name	Calcination strategies	Nomenclature
Co-doped Cu_1Mn_8	Stagnant air	$3\%CoCuMn_8Ox_{SA}$
	Flowing air	$3\%CoCuMn_8Ox_{FA}$
	Reactive calcination	$3\%CoCuMn_8Ox_{RC}$
Ce-doped Cu_1Mn_8	Stagnant air	$3\%CeCuMn_8Ox_{SA}$
	Flowing air	$3\%CeCuMn_8Ox_{FA}$
	Reactive calcination	$3\%CeCuMn_8Ox_{RC}$
Ag-doped Cu_1Mn_8	Stagnant air	$3\%AgCuMn_8Ox_{SA}$
	Flowing air	$3\%AgCuMn_8Ox_{FA}$
	Reactive calcination	$3\%AgCuMn_8Ox_{RC}$
Fe-doped Cu_1Mn_8	Stagnant air	$3\%FeCuMn_8Ox_{SA}$
	Flowing air	$3\%FeCuMn_8Ox_{FA}$
	Reactive calcination	$3\%FeCuMn_8Ox_{RC}$

7.2 Catalyst Characterization

Characterization of doped and un-doped Cu_1Mn_8 catalysts prepared in reactive calcination (RC) conditions was done by the different techniques and their activity for CO oxidation was discussed below:

7.2.1 XRD analysis

The phase identification and cell dimensions of various doped Cu_1Mn_8 catalyst was done by the X-ray powder diffraction (XRD) technique. The XRD analysis of Cu_1Mn_8 catalyst doping with (3wt.%) Co, Ce, Fe, and Ag were individually provides information about the crystallite size and coordinate dimensions present in the catalysts. XRD pattern of all the catalysts was displayed in Figure 7.2. In $3\%CoCuMn_8Ox_{RC}$ catalyst, the diffraction peak at 2θ was 32.50 and structure was Face-centered $Cu_{0.5}Mn_{3.5}CoO_4$ phase. The crystallite size of catalyst was 3.90nm. In $3\%FeCuMn_8Ox_{RC}$ catalyst, the diffraction peak at 2θ was 33.12 and the structure was Face-centered cubic $Cu_{0.5}Mn_{2.5}Fe_2O_4$ phase. The crystallite size of catalyst was 3.65nm.

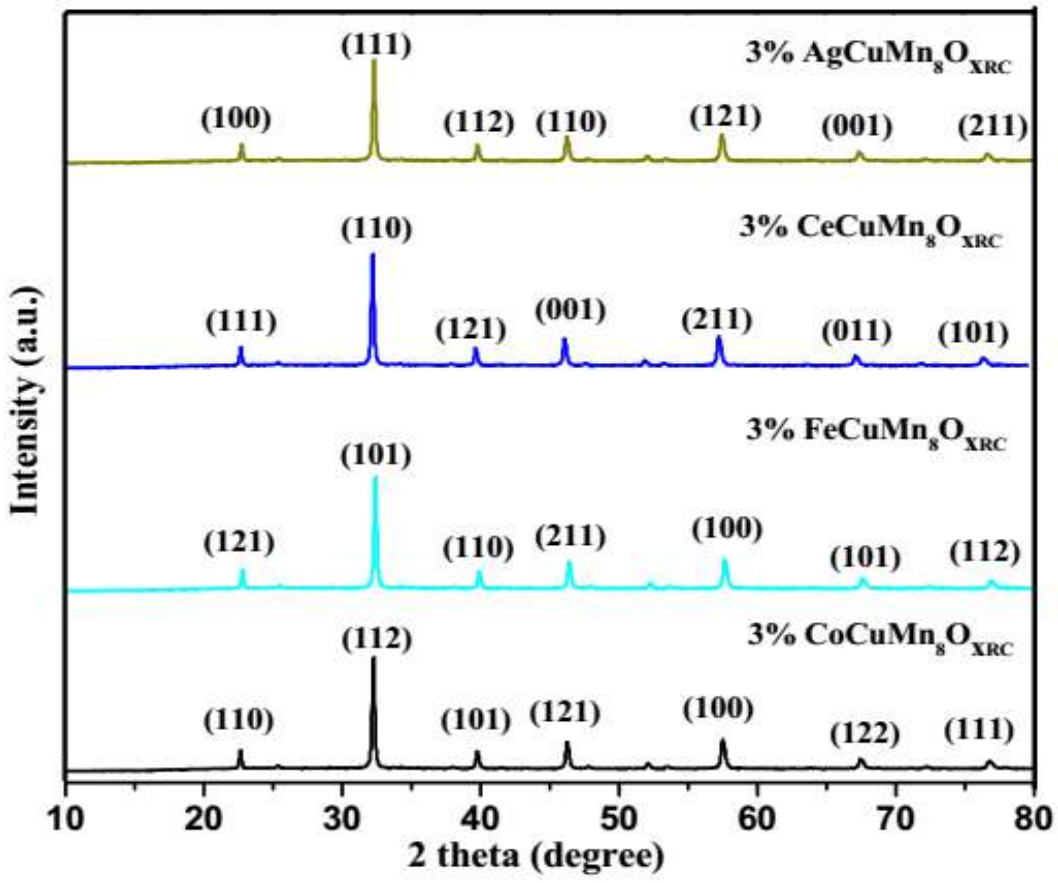

Figure 7.2: XRD analysis of Cu_1Mn_8 catalyst doped with Co, Ce, Fe and Ag

In $3\%CeCuMn_8Ox_{RC}$ catalyst, the diffraction peak at 2θ was 32.58 and the structure was Face-centered cubic $Ce(Cu_{0.2}Mn_{1.6}O)$ phase with crystallite size of catalyst was 2.90nm.

In 3%$AgCuMn_8Ox_{RC}$ catalyst, the diffraction peak at 2θ was 32.60 and structure was Face centered cubic $Cu_{0.4}Mn_3(AgO)$ phase with crystallite size of catalyst was 2.40nm. After XRD analysis we can confirmed that the crystallite size of 3%$AgCuMn_8Ox_{RC}$ catalyst was slightly lower than other catalysts so that it performs better activity for CO oxidation at a lower temperature. Refinement of XRD pattern of 3%$AgCuMn_8Ox_{RC}$ catalyst sample shows that there will be no impurity phases were present in the catalyst. The crystallite size of particles present in catalysts was as follows: 3%$CoCuMn_8Ox_{RC}$ > 3%$FeCuMn_8Ox_{RC}$ > 3%$CeCuMn_8Ox_{RC}$ > 3%$AgCuMn_8Ox_{RC}$. The highest crystallite size was found in 3%$CoCuMn_8Ox_{RC}$ catalyst. The 3%$AgCuMn_8Ox_{RC}$ catalyst was a lowest crystalline size therefore we found to possess high catalytic activity for low-temperature CO oxidation. From XRD analysis we confirm that the doped material uniformly dispersed on the surface of CuMnOx catalyst.

7.2.2 FTIR analysis

The metal-oxygen bonds present in the doped Cu_1Mn_8 catalysts was analysis by the Fourier transform infrared spectroscopy (FTIR) techniques. The different peaks are shows various types of chemical groups present in the Cu_1Mn_8 catalysts. The FTIR transmission spectrum in the region (4000–400cm^{-1}) of the Cu_1Mn_8 catalysts prepared by reactive calcination (RC) conditions was shown in Figure 7.3. In 3%$CoCuMn_8Ox_{RC}$ catalyst, the MnO_2 vibration mode was observed at 1640cm^{-1} due to the stretching of Mn-O bond. The transmission spectra 1330cm^{-1} is showed CuO group, 2920cm^{-1} is showed Co_3O_4 group and 3530cm^{-1} is showed -OH group [Hasegawa *et al.,* 2009]. In 3%$CeCuMn_8Ox_{RC}$ catalyst at the transmittance conditions there are total four peaks obtained. The IR brand 1640cm^{-1} is showed the stretching Mn-O bond, 3490cm^{-1} is showed -OH group, 1180cm^{-1} is showed CuO group and 2140cm^{-1} is showed CeO_2 group. In 3%$AgCuMn_8Ox_{RC}$ catalyst at the transmittance conditions there are total four

peaks obtained, the IR band 1540cm^{-1} have shown the presence of MnO_2 group, 3530cm^{-1} is showed -OH group, 640cm^{-1} is showed CuO group and 1280cm^{-1} is showed AgO_2 group [Guo *et al.,* 2016]. In 3%FeCuMn$_8$Ox$_{RC}$ catalyst, at the transmittance conditions there are total six peaks obtained, the IR band 3490cm^{-1} have shown the presence of -OH group and band (1640cm^{-1} and 1060 cm^{-1}) is show Mn-O band. The other band 2340cm^{-1} has shown the presence of FeO_2 band, 640cm^{-1} is showed CuO group and 1180cm^{-1} is showed CO_3^{2-} group. These results show that the 3%FeCuMn$_8$Ox$_{RC}$ catalyst consist of carbonate species. The FTIR investigate produce the surface chemistry and reactivity of different catalysts [Cai *et al.,* 2012].

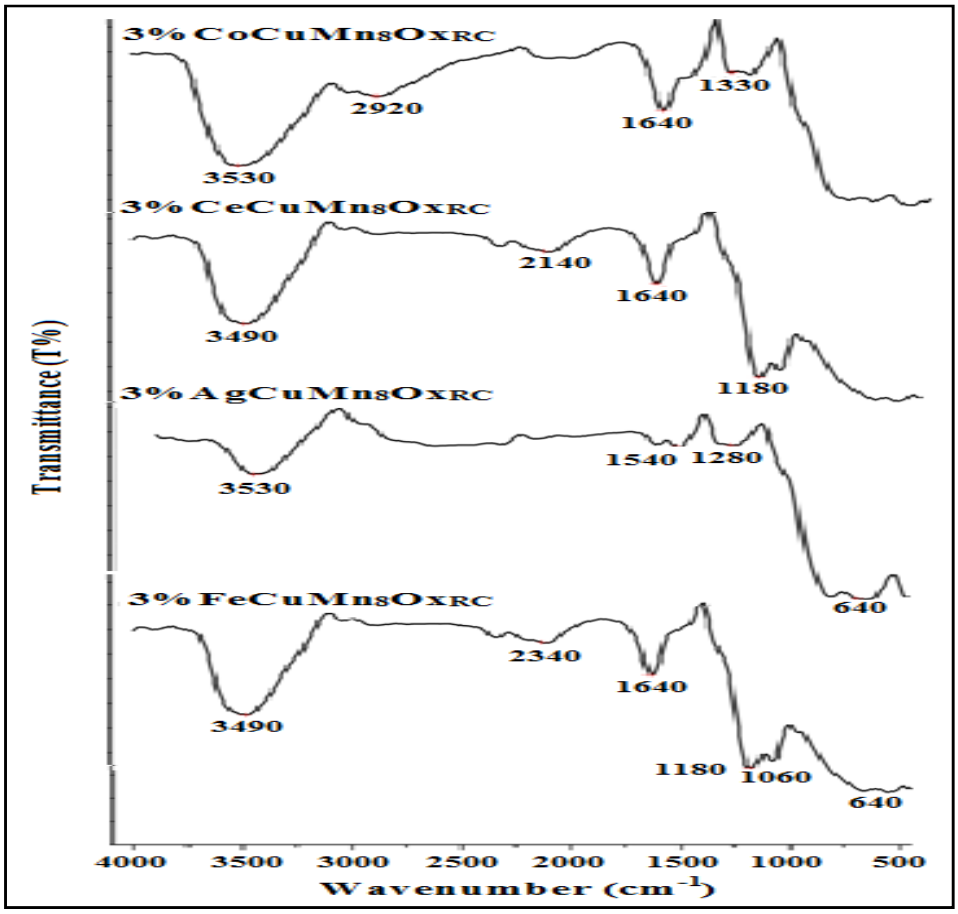

Figure 7.3: FTIR analysis of the catalyst

From FTIR analysis observed that the spectra of impurities decrease in the following order: 3%CoCuMn$_8$Ox$_{RC}$> 3%FeCuMn$_8$Ox$_{RC}$> 3%CeCuMn$_8$Ox$_{RC}$> 3%AgCuMn$_8$Ox$_{RC}$. Thus, the 3%AgCuMn$_8$Ox$_{RC}$ catalyst has shown that the highest purity as compared to the other catalysts.

7.2.3 SEM analysis

Textural property of the different doped Cu_1Mn_8 catalysts was analyzed by the scanning electron microscopy (SEM). It can be seen that the particles present in Cu_1Mn_8 catalysts was crystalline form. All catalysts were prepared in reactive calcination conditions. They show granular particles between 0.5 and 4µm calculated by "image j software" with varying degree of agglomeration. As seen in the SEM micrograph, the particles were comprised of more coarse, coarse, fine and finest size grains resulted by RC of 3%CoCuMn$_8$Ox$_{RC}$, 3%FeCuMn$_8$Ox$_{RC}$, 3%CeCuMn$_8$Ox$_{RC}$ and 3%AgCuMn$_8$Ox$_{RC}$ catalyst respectively. The particle size of 3%CoCuMn$_8$Ox$_{RC}$ catalyst was relatively larger and agglomerated as compared to the other catalysts. Thus, the different dopent present in Cu_1Mn_8 catalyst has much affect on the porosity, particle size and morphology of the resulting catalysts.

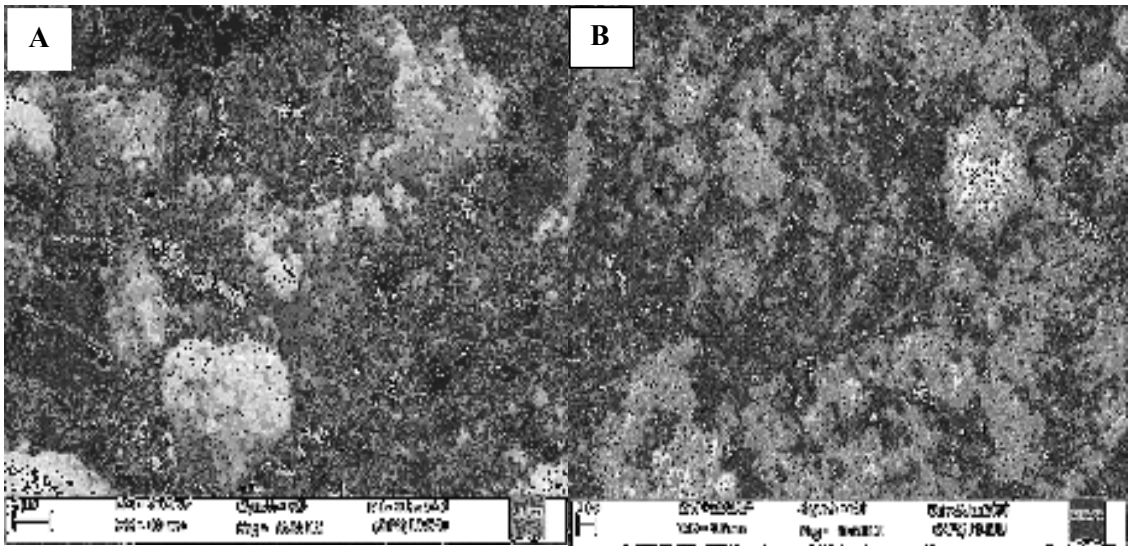

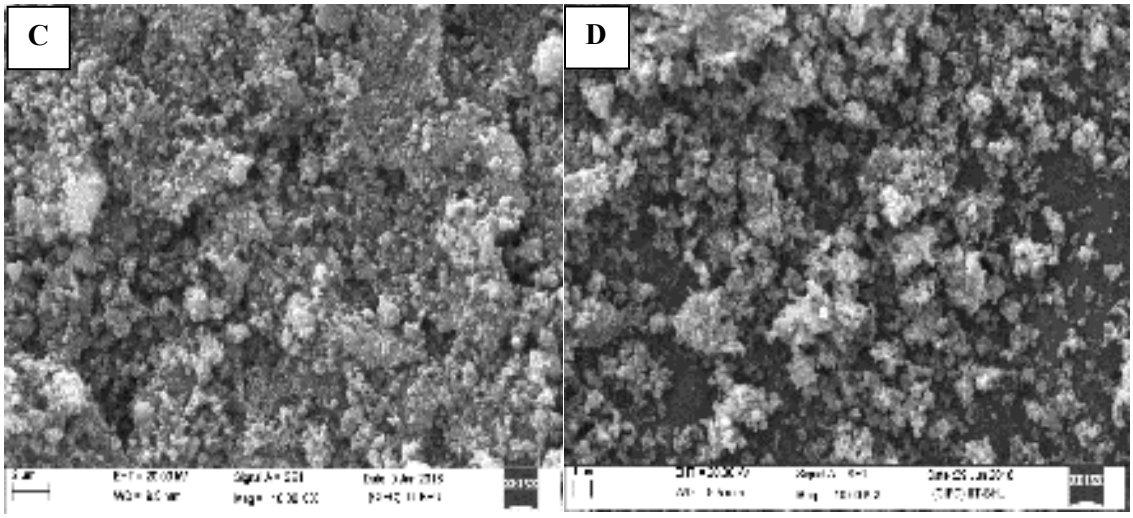

Figure 7.4: SEM image of (A) 3%CoCuMn$_8$Ox$_{RC}$, (B) 3%FeCuMn$_8$Ox$_{RC}$, (C) 3%CeCu Mn$_8$Ox$_{RC}$ and (D) 3%AgCuMn$_8$Ox$_{RC}$

Figure 7.4 shows that the doping materials were uniformly distributed in the micrometer range over the Cu_1Mn_8 catalyst surface despite of the reaction temperature. The synergetic effect of Cu_1Mn_8 catalyst extremely depends upon the catalyst composition and the nature of oxidized compounds.

7.2.4 SEM-EDX analysis

In the doped Cu_1Mn_8 catalysts, the percentages of different elements were present analysis by the energy dispersive X-ray (EDX) analysis. The results of energy dispersive X-ray analysis (EDX) have shown that all the catalyst samples were pure due to the presence of their relative element peaks only.

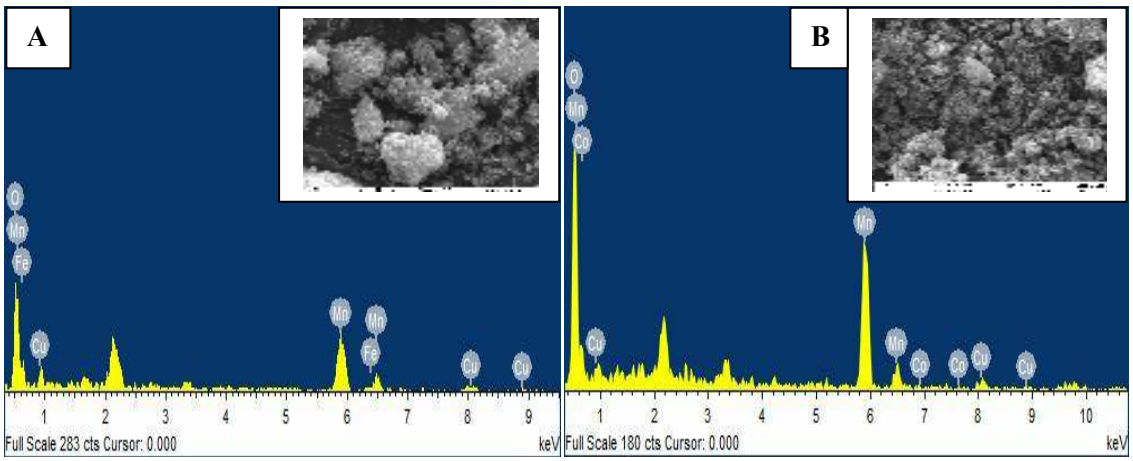

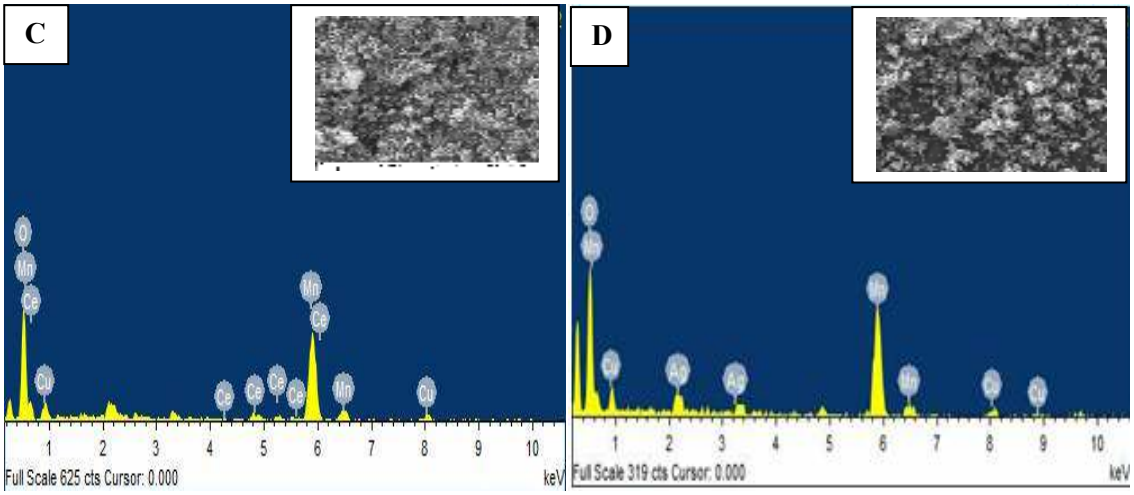

Figure 7.5: SEM-EDX image of (A) 3%$FeCuMn_8Ox_{RC}$, (B) 3%$CoCuMn_8Ox_{RC}$, (C) 3%$CeCuMn_8Ox_{RC}$ and (D) 3%$AgCuMn_8Ox_{RC}$ catalysts

The SEM-EDX image of doped Cu_1Mn_8 catalysts has shown in Figure 7.5. Atomic percentage of Fe, Ag, Ce and Co element in the 3%$FeCuMn_8Ox_{RC}$, 3%$AgCuMn_8Ox_{RC}$, 3%$CeCuMn_8Ox_{RC}$ and 3%$CoCuMn_8Ox_{RC}$ catalyst was 2.72%, 2.30%, 2.38% and 2.20% respectively. The oxygen present in 3%$AgCuMn_8Ox_{RC}$ catalyst was least as compared to the other catalysts. The high amounts of surface chemisorbed oxygen presents in 3%$AgCuMn_8Ox_{RC}$ catalyst was highly preferable for CO oxidation.

Table 7.2: Atomic percentage of dopant in Cu_1Mn_8 catalyst by EDX analysis

3%$CoCuMn_8Ox_{RC}$	**Cu**	**Mn**	**O**	**Co**
Atomic percentage	2.70	22.45	72.65	2.20
3%$CeCuMn_8Ox_{RC}$	**Cu**	**Mn**	**O**	**Ce**
Atomic percentage	3.48	32.09	62.05	2.38
3%$AgCuMn_8Ox_{RC}$	**Cu**	**Mn**	**O**	**Ag**
Atomic percentage	9.82	29.22	58.66	2.30
3%$FeCuMn_8Ox_{RC}$	**Cu**	**Mn**	**O**	**Fe**
Atomic percentage	4.69	20.30	72.29	2.72

The atomic percentage of oxygen present in the doped Cu_1Mn_8 catalyst was decreased in the following order: $3\%AgCuMn_8Ox_{RC}$> $3\%CeCuMn_8Ox_{RC}$> $3\%FeCuMn_8Ox_{RC}$> $3\%CoCuMn_8Ox_{RC}$. This indicates that the presence of oxygen deficit in the $3\%AgCuMn_8Ox_{RC}$ catalyst which makes the high density of active sites. The doping materials associated with Cu_1Mn_8 catalyst promote their oxygen storage capacity and release improved their oxygen mobility. A calcination strategy of the $3\%AgCuMn_8Ox_{RC}$ catalyst has highly influenced the elemental distribution of different elements presents in the catalyst surfaces. The existence of pure oxides phase on the catalyst surfaces was also a good harmony with the XRD and FTIR results also.

7.2.5 Surface area measurement

The surface area of all doped Cu_1Mn_8 catalyst was analysis by the Brunauer-Emmett-Teller analysis (BET). The pore volume, surface area and pore size of all the catalyst samples prepared in reactive calcination was represented in the Table.7.3. It can be visualized from the table that the pore volume and pore size of $3\%AgCuMn_8Ox$ catalyst was much superior to the other catalysts. The average pore volume and pore size of $3\%AgCuMn_8Ox$ catalyst was $0.776cm^3/g$ and 68.45Å respectively. The prepared samples exhibited hysteresis loop, which indicated that the pores were exhibiting geometries of mesopores. The textural properties doped Cu_1Mn_8 catalyst was shown in the Figure 7.6. The existence of hysteresis loop at a relative pressure (P/P_0) of 0.6–1.0 indicates that the porosity arising from the non-crystalline intra-aggregate voids and spaces formed by inter-particle contacts.

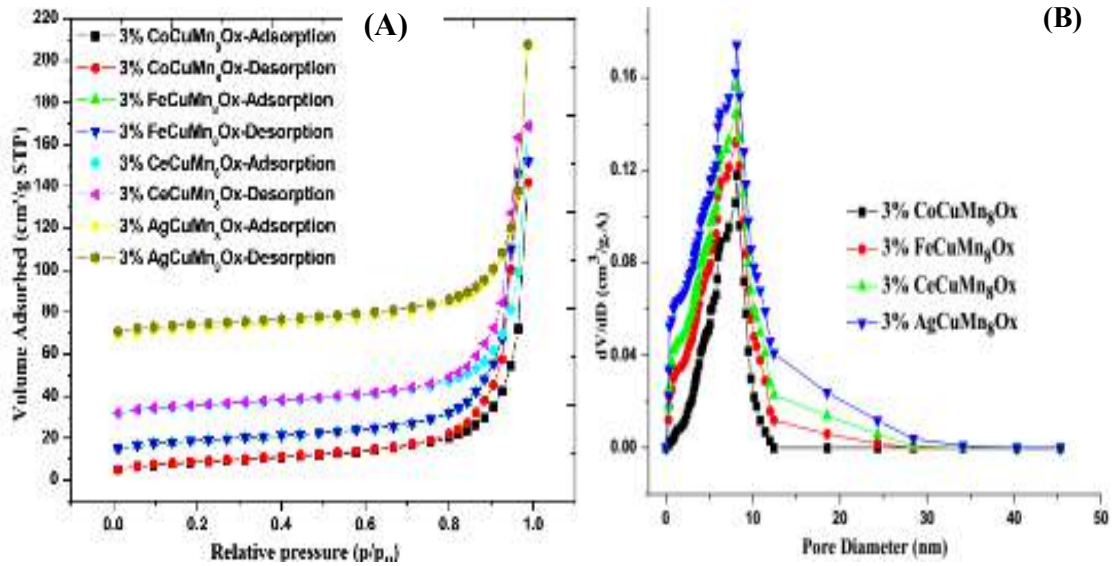

Figure 7.6: Textural properties (A) N_2 adsorption-desorption isotherms and (B) Pore size distribution

Figure 7.6(B) shows that the pore size distributions (PSDs) from the desorption branch of the nitrogen isotherms. Total pore volume and specific surface area were two major factors which can influence the catalytic activity for CO oxidation. Clearly, the textural property of $3\%AgCuMn_8Ox_{RC}$ catalyst was greater active for CO oxidation at a low temperature.

Table 7.3: Textural property of the catalysts

Catalyst	Surface Area (m^2/g)	Pore Volume (cm^3/g)	Ave. Pore Size (Å)
$3\%AgCuMn_8Ox_{RC}$	145.76	0.776	68.45
$3\%CeCuMn_8Ox_{RC}$	137.35	0.743	76.50
$3\%FeCuMn_8Ox_{RC}$	129.37	0.710	88.45
$3\%CoCuMn_8Ox_{RC}$	122.65	0.675	94.65

The doping of silver into Cu_1Mn_8 catalyst resulted in a specific surface area and total pore volume of 3%$AgCuMn_8Ox_{RC}$ catalyst. The surface area of 3%$AgCuMn_8Ox_{RC}$, 3%$CeCuMn_8Ox_{RC}$, 3%$FeCuMn_8Ox_{RC}$ and 3%$CoCuMn_8Ox_{RC}$ catalyst was 145.76, 137.35, 129.37 and 122.65m^2/g respectively. Typical nitrogen adsorption/desorption isotherms of these catalysts with hysteresis loop showing catalysts were meso-porous according to De-Boer classification. In the mesopores, molecules from a liquid-like adsorbed phase having a meniscus of which curvature was related with the Kelvin equation, providing the pore size distribution calculation. The 3%$AgCuMn_8Ox_{RC}$ catalyst surface area (145.76m^2/g) and pore volume (0.776cm^3/g) was so high so that it was most active for CO oxidation at a low temperature. When the activity was tested (see later), it was observed that the higher catalyst surface area and total volume resulted in the greatest catalytic activity. The specific surface area was measured by BET analysis and it was also follows the SEM and XRD results.

7.3 Catalyst performance and activity measurement

The addition of different promoters like (Co, Ce, Ag and Fe) into the Cu_1Mn_8 catalyst to improved their performance for CO oxidation. Activity of the various doped and un-doped Cu_1Mn_8 catalyst was done in different calcinations conditions, like reactive calcination (RC), flowing air calcination (FAC) and stagnant air calcination (SAC) conditions into the laboratory. The activity test was carried out to compare the efficiency of various doped Cu_1Mn_8 catalysts produced by different conditions for CO oxidation.

7.3.1 Effect of promoters on the activity of Cu_1Mn_8 catalysts produced under stagnant air calcination

The effect of promoters on activity of Cu_1Mn_8 catalysts produced under stagnant air calcination conditions for CO oxidation is shown in the Figure 7.7. The lights of characteristics of the catalysts were used to compare the activity, which are tabulated in Table 7.4. The 10% conversion of CO over the un-doped Cu_1Mn_8 and doped $3\%AgCuMn_8Ox_{SA}$, $3\%CeCuMn_8Ox_{SA}$, $3\%FeCuMn_8Ox_{SA}$ and $3\%CoCuMn_8Ox_{SA}$ catalysts were 35ºC, 30ºC, 30ºC, 25ºC and 28ºC respectively (Figure 7.7). The 50% conversion of CO over the un-doped Cu_1Mn_8 and doped $3\%AgCuMn_8Ox_{SA}$, $3\%CeCuMn_8Ox_{SA}$, $3\%FeCuMn_8Ox_{SA}$ and $3\%CoCuMn_8Ox_{SA}$ catalysts were 102ºC, 65ºC, 68ºC, 75ºC and 85ºC respectively.

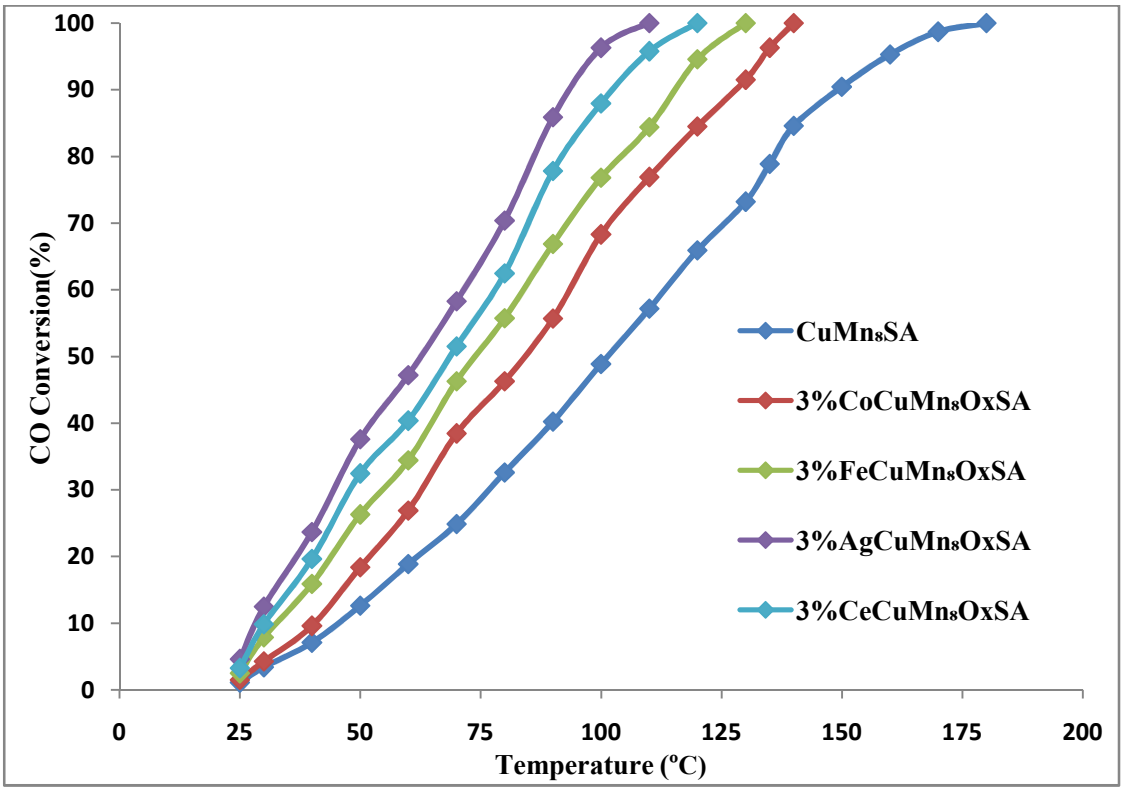

Figure 7.7: Catalytic activity of doped and un-doped Cu_1Mn_8 catalysts produced by calcination in stagnant air

The total conversion of CO over the Cu_1Mn_8, 3%$AgCuMn_8Ox_{SA}$, 3%$CeCuMn_8Ox_{SA}$, 3%CoCu Mn_8Ox_{SA}, 3%$FeCuMn_8Ox_{SA}$ catalysts were 178°C, 112°C, 118°C, 128°C, and 141°C respectively. It is clear from the Table 7.4 and Figure 7.7 that, all the promoted catalysts show better activity than the unprompted Cu_1Mn_8 catalyst. The total conversion of CO over 3%$AgCuMn_8Ox_{SA}$ catalyst occurred at the lowest temperature of 118°C. The total conversion of CO over un-promoted $CuMn_8$ catalyst occurred at the highest temperature of 178°C. Thus, the order of activity of the catalysts for CO oxidation is as follows: 3%$AgCuMn_8Ox_{SA}$> 3%$CeCuMn_8Ox_{SA}$> 3%$FeCuMn_8Ox_{SA}$> 3%$CoCuMn_8Ox_{SA}$> Cu_1Mn_8. There is a difference of 66°C temperature of the total oxidation of CO for un-doped Cu_1Mn_8 and silver doped Cu_1Mn_8 catalyst.

Table 7.4: Light off characteristics of catalysts for CO oxidation in stagnant air

Catalyst	**T_{10}**	**T_{50}**	**T_{100}**
Cu_1Mn_{8SA}	35ºC	102ºC	178ºC
3%$CoCuMn_8Ox_{SA}$	30ºC	85ºC	141ºC
3%$FeCuMn_8Ox_{SA}$	30ºC	75ºC	128ºC
3%$AgCuMn_8Ox_{SA}$	25ºC	65ºC	112ºC
3%$CeCuMn_8Ox_{SA}$	28ºC	68ºC	118ºC

The relative favorable textural properties of highest surface area, open textured pores, smallest crystallite size and smallest particle size of the 3%$AgCuMn_8Ox$ catalyst favor for easy diffusion of reactants and products and thus assist the oxidation process. Therefore, it can be summarized that the addition of silver into the Cu_1Mn_8 catalyst influenced their activity for CO oxidation.

7.3.2 Effect of promoters on activity of Cu_1Mn_8 catalysts produced under flowing air calcination

It is evident from Figure 7.8 and light off characteristics Table 7.5 that T_{10} i.e. the 10% conversion of CO over the un-doped Cu_1Mn_8 and doped 3%$AgCuMn_8Ox_{FA}$, 3%$CeCuMn_8Ox_{FA}$, 3%$FeCuMn_8Ox_{FA}$ and 3%$CoCuMn_8Ox_{FA}$ catalysts were 32ºC, 25ºC, 26ºC, 28ºC and 30ºC respectively. In the initial conditions, a very slow exothermic reaction for CO oxidation was going on over the catalyst, it causes rising in the local temperature. The T_{50} over the un-doped Cu_1Mn_8 and doped 3%$AgCuMn_8Ox_{FA}$, 3%$CeCuMn_8Ox_{FA}$, 3%$FeCuMn_8Ox_{FA}$ and 3%$CoCuMn_8Ox_{FA}$ catalysts were 73ºC, 52ºC, 57ºC, 61ºC and 66ºC respectively.

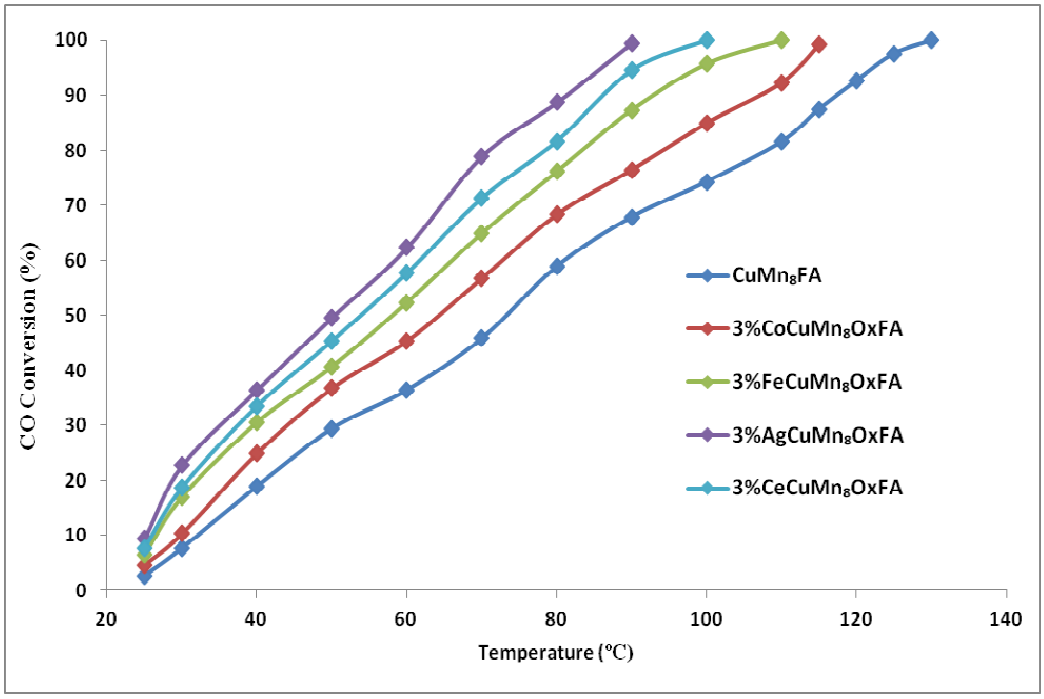

Figure 7.8: Catalytic activity of doped and un-doped Cu_1Mn_8 catalysts produced in flowing air

The T_{100} over the Cu_1Mn_8, 3%$AgCuMn_8Ox_{FA}$, 3%$CeCuMn_8Ox_{FA}$, 3%$CoCuMn_8Ox_{FA}$, 3%$FeCuMn_8Ox_{FA}$ catalysts were 128°C, 88°C, 98°C, 112°C, and 115°C respectively. Thus, the order of activity of the catalysts for CO oxidation is as follows: $3\%AgCuMn_8Ox_{FA}>3\%CeCuMn_8Ox_{FA}>3\%FeCuMn_8Ox_{FA}>3\%CoCuMn_8Ox_{FA}>Cu_1Mn_8$.

Table 7.5: Light off characteristics of catalysts for CO oxidation in flowing air

Catalyst	T_{10}	T_{50}	T_{100}
Cu_1Mn_8	32ºC	73ºC	128ºC
$3\%CoCuMn_8Ox_{FA}$	30ºC	66ºC	115ºC
$3\%FeCuMn_8Ox_{FA}$	28ºC	61ºC	112ºC
$3\%AgCuMn_8Ox_{FA}$	25ºC	52ºC	88ºC
$3\%CeCuMn_8Ox_{FA}$	26ºC	57ºC	98ºC

There is a difference of 40°C for the total oxidation of CO for un-doped Cu_1Mn_8 and silver doped $3\%AgCuMn_8Ox_{FA}$ catalyst. The improved catalytic activity of the 3%Ag $CuMn_8Ox_{FA}$ catalyst can be ascribed to the unique structural, textural chacateristics and the least crystallite size. Clearly, doped catalysts showed better activity than un-doped catalyst. Catalyst formulation $3\%AgCuMn_8Ox_{FA}$ resulted the maximum activity for CO oxidation. The occurrence of highly disperse and more specific surface area in the $3\%AgCuMn_8Ox_{FA}$ catalyst favoured for CO oxidation.

7.3.3 Effect of promoters on activity of Cu_1Mn_8 catalysts produced under reactive calcination

In initially, a very slow exothermic oxidation of CO over the precursor's crystallites started causing a small rise in the local temperature, ensuing decomposition of the precursor also. The 10% conversion of CO over the un-doped Cu_1Mn_8 and doped $3\%AgCuMn_8Ox_{RC}$, $3\%CeCuMn_8Ox_{RC}$, $3\%FeCuMn_8Ox_{RC}$ and $3\%CoCuMn_8Ox_{RC}$ catalysts were 28ºC, 25ºC, 26ºC, 27ºC and 28ºC respectively.

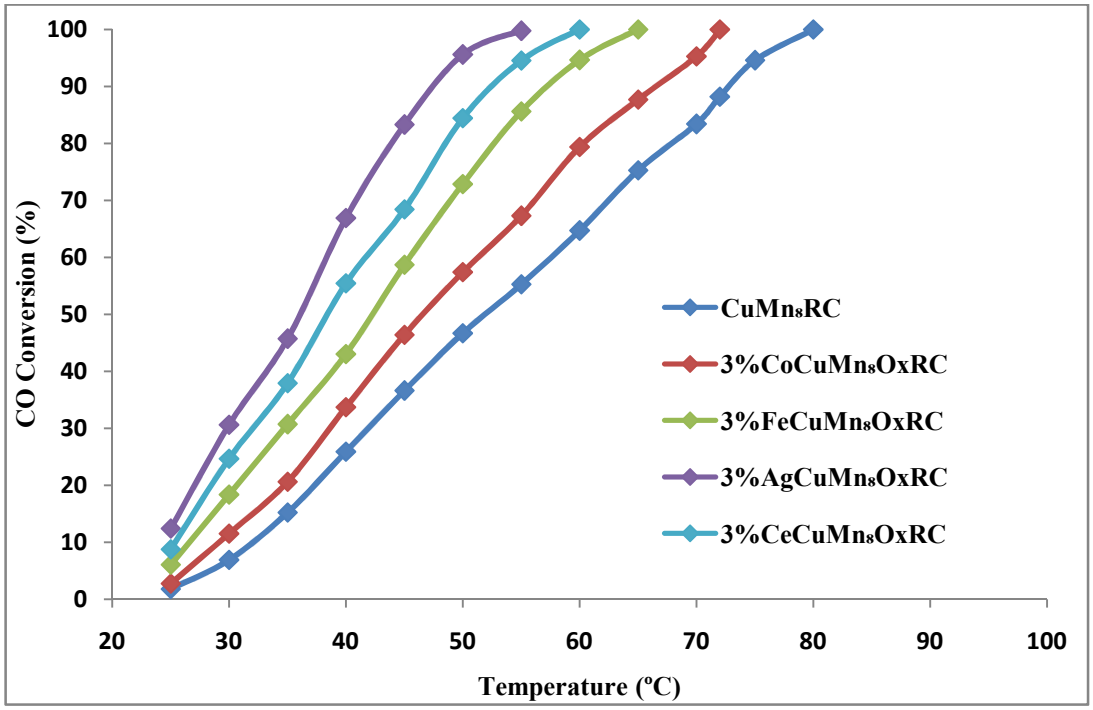

Figure 7.9: Catalytic activity of doped and un-doped Cu_1Mn_8 catalysts produced by reactive calcination

The 50% conversion of CO over the un-doped Cu_1Mn_8 and doped $3\%AgCuMn_8Ox_{RC}$, $3\%CeCuMn_8Ox_{RC}$, $3\%FeCuMn_8Ox_{RC}$ and $3\%CoCuMn_8Ox_{RC}$ catalysts were 51°C, 36°C, 39°C, 42°C and 48°C respectively. The total conversion of CO over the Cu_1Mn_8, $3\%AgCuMn_8Ox_{RC}$, $3\%CeCuMn_8Ox_{RC}$, $3\%CoCuMn_8Ox_{RC}$, $3\%FeCuMn_8Ox_{RC}$ catalysts were 78°C, 54°C, 58°C, 72°C and 64°C respectively.

Table 7.6: Light off characteristics of catalysts for CO oxidation in reactive calcination

Catalyst	T_{10}	T_{50}	T_{100}
Cu_1Mn_8	28°C	50°C	80°C
$3\%CoCuMn_8Ox_{RC}$	25°C	48°C	72°C
$3\%FeCuMn_8Ox_{RC}$	26°C	42°C	65°C
$3\%AgCuMn_8Ox_{RC}$	27°C	35°C	54°C
$3\%CeCuMn_8Ox_{RC}$	28°C	40°C	60°C

The 3%AgCuMn$_8$Ox$_{RC}$ catalyst has shown the best performance for CO oxidation at a low temperature and these systems were now worthy for further investigation. This result demonstrated that the doped and un-doped Cu_1Mn_8 catalysts prepared by reactive calcination conditions were very active for complete oxidation of CO at temperature range between 54–78°C.

7.3.4 Comparison of reactive calcination with traditional calcination of catalyst precursors

A comparative study of CO oxidation over the 3%AgCuMn$_8$Ox catalyst produced under various calcination conditions of stagnant air, flowing air and RC is shown in Figure 7.10. It is evident that the calcination strategies of the precursors have a great influence on the activity of resulting catalysts. At 25^{o}C the conversion of CO over the 3%AgCuMn$_8$Ox$_{SA}$, 3%AgCuMn$_8$Ox$_{FA}$ and 3%AgCuMn$_8$Ox$_{RC}$ catalysts produced under different calcination strategies were 12%, 15% and 23% respectively.

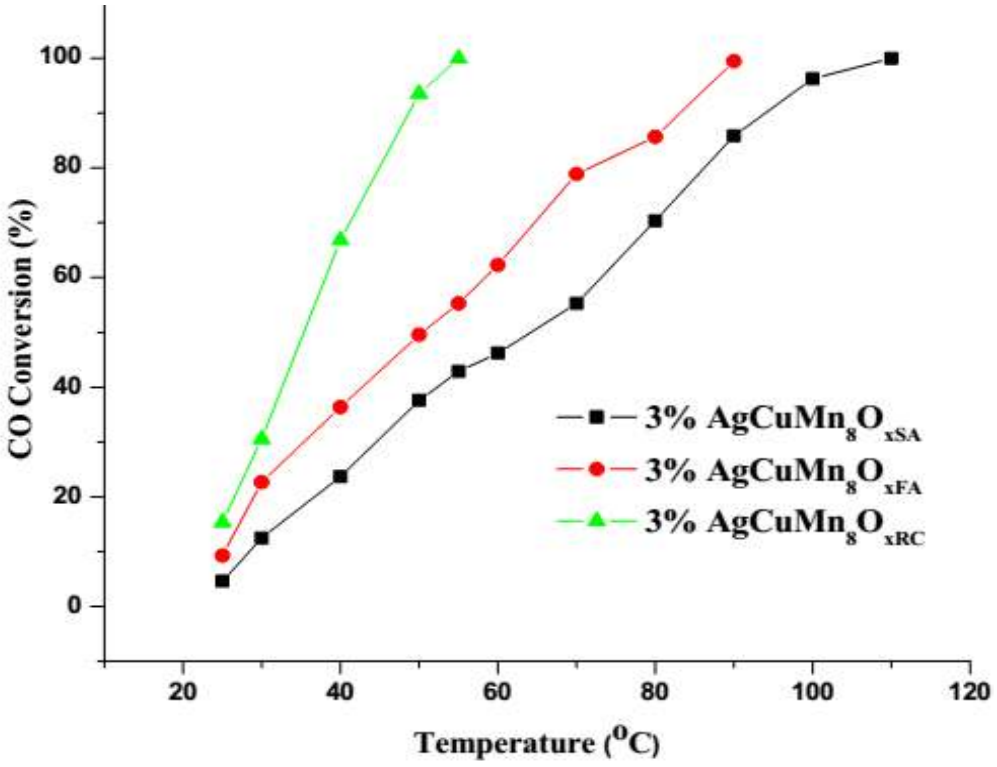

Figure 7.10: Activity test of 3%AgCuMn$_8$Ox catalysts under different calcination conditions

The 50% conversion of CO over the 3%AgCuMn$_8$Ox$_{RC}$ catalyst was 35°C, which was lowered by 30°C and 17°C over than that of 3%AgCuMn$_8$Ox$_{SA}$ and 3%AgCuMn$_8$Ox$_{FA}$ catalysts respectively. The total conversion of CO was 55ºC over 3%AgCuMn$_8$Ox$_{RC}$ catalyst, which was lowered by 57°C and 27°C over than that of 3%AgCuMn$_8$Ox$_{SA}$ and 3%AgCuMn$_8$Ox$_{FA}$ catalysts respectively. The activity order for CO oxidation in the decreasing sequence was as follows: 3%AgCuMn$_8$Ox$_{RC}$> 3%AgCuMn$_8$Ox$_{FA}$> 3%AgCu Mn$_8$Ox$_{SA}$.

Table 7.7: Light-off characteristics of 3%AgCuMn$_8$Ox catalysts

Catalyst	**T_{50}**	**T_{100}**
3%AgCuMn$_8$Ox$_{SA}$	65ºC	112ºC
3%AgCuMn$_8$Ox$_{FA}$	52ºC	82ºC
3%AgCuMn$_8$Ox$_{RC}$	35ºC	55ºC

The occurrence of partially reduced phases creates an oxygen deficient defective structure which provides a high density of active sites as a result of reactive calcination, consequently the 3%AgCuMn$_8$Ox$_{RC}$ turn into the most active catalyst. Finally, we get that the RC route was the most appropriated calcination strategy for the production of highly active 3%AgCuMn$_8$Ox$_{RC}$ catalyst for CO oxidation.

7.3.5 Optimization of silver doping in Cu_1Mn_8 catalyst

The catalytic activity of Ag doped Cu_1Mn_8 depends upon the silver loading (wt.%): the overall activity for CO oxidation was increased as the silver percentage increase from 1 to 3 wt%, and then decrease with a further increase in loading up to 5wt%. The trend of activity of the catalysts was in accordance with XRD, surface area and SEM results emphasizing that smaller crystallite size, as well as particle size, higher surface area,

and easy reducibility, produce an efficient catalyst for CO oxidation. The oxidation of CO was initiated in RC conditions at ~25°C overall all the catalyst samples and 50% conversion of CO over the 3%AgCuMn$_8$Ox$_{RC}$ catalyst was 35°C temperature, which was less by 20°C, 15°C, 10°C, 5°C and 8°C over than that of Cu_1Mn_8, 1%AgCu Mn$_8$Ox$_{RC}$, 2%AgCuMn$_8$Ox$_{RC}$, 4%AgCuMn$_8$Ox$_{RC}$ and 5%AgCuMn$_8$Ox$_{RC}$ catalysts respectively. The total conversion of CO was 55ºC over 3%AgCuMn$_8$Ox$_{RC}$ catalyst, which was less by 25°C, 20°C, 15°C, 5°C and 10°C over than that of CuMn$_8$Ox$_{RC}$, 1%AgCuMn$_8$Ox$_{RC}$, 2%AgCuMn$_8$Ox$_{RC}$, 4%AgCuMn$_8$Ox$_{RC}$ and 5%AgCu Mn$_8$Ox$_{RC}$ catalysts respectively. The exothermic initiation oxidation of CO rising the local point temperature of the catalyst higher than the measured bulk temperature. The silver promotion has improved the stability of Cu_1Mn_8 catalyst and they create an ideal condition for the catalyst.

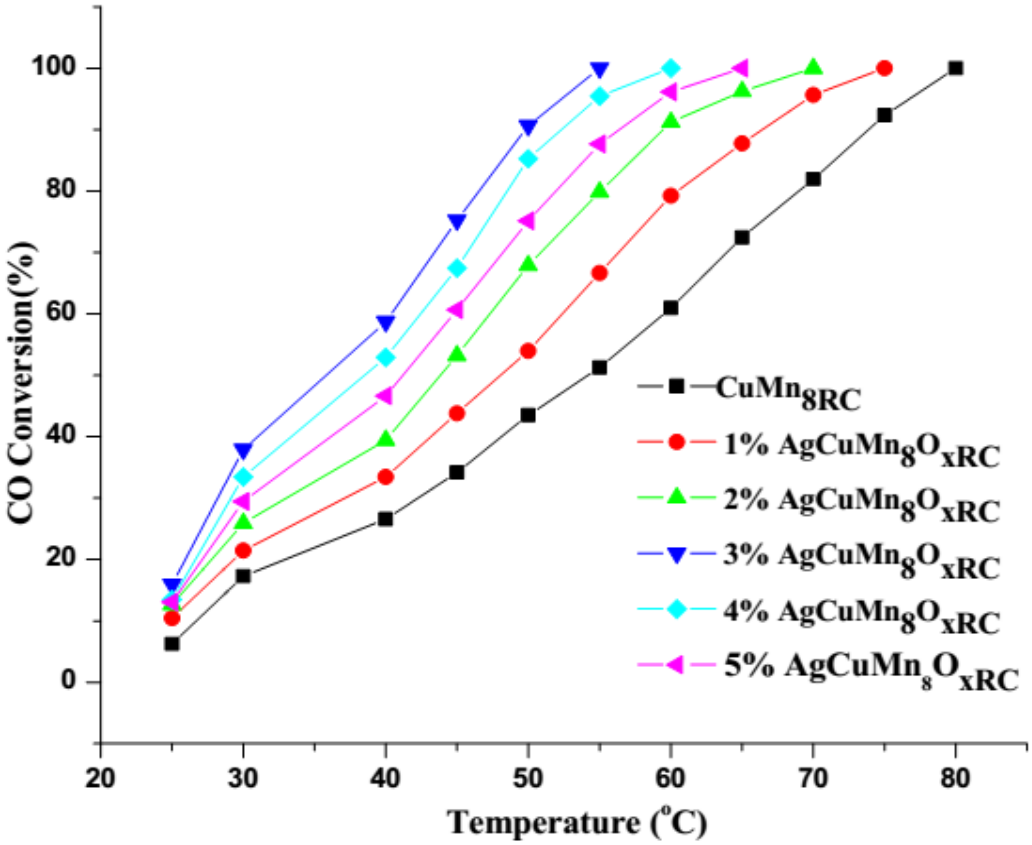

Figure 7.11: Optimization of silver doping in Cu_1Mn_8

Table 7.8: Optimization of wt.% Ag in Cu_1Mn_8

Catalyst	**T_{50}**	**T_{100}**
Cu_1Mn_{8RC}	55ºC	80ºC
$1\%AgCuMn_8Ox_{RC}$	50ºC	75ºC
$2\%AgCuMn_8Ox_{RC}$	45ºC	70ºC
$3\%AgCuMn_8Ox_{RC}$	35ºC	55ºC
$4\%AgCuMn_8Ox_{RC}$	40ºC	60ºC
$5\%AgCuMn_8Ox_{RC}$	43ºC	65ºC

The order of activity of different types of catalysts for CO oxidation was as follows: $3\%AgCuMn_8Ox_{RC}$>$4\%AgCuMn_8Ox_{RC}$>$2\%AgCuMn_8Ox_{RC}$>$5\%AgCuMn_8Ox_{RC}$>1%Ag $CuMn_8Ox_{RC}$>Cu_1Mn_8. After the activity test, we can confirm that the 3%AgCu Mn_8Ox_{RC} catalyst has a higher catalytic activity for CO oxidation as compared to the other catalysts. The extraordinary performance of $3\%AgCuMn_8Ox_{RC}$ catalyst prepared by RC conditions for CO oxidation was associated with the modification in intrinsic textural, morphological characteristics such as crystallite size, surface area and particle size of the catalyst.

7.4 Concluding Remarks

The CO oxidation over various types of doped and un-doped Cu_1Mn_8 catalyst is highly influenced by the surface area, pore volume and crystalline of the catalyst. From the results and discussions, we can confirm that the addition of different promoters into the Cu_1Mn_8 catalysts to improve their performance for CO oxidation. It is propose that the Cu_1Mn_8 catalyst doping with silver oxide have a higher catalytic activity as compared to the other catalysts. The order of activity for different types of doped and un-doped

Cu_1Mn_8 catalyst for CO oxidation is as follows: 3%AgCuMn$_8$Ox>3%CeCuMn$_8$Ox >3%FeCuMn$_8$Ox>3%CoCuMn$_8$Ox>Cu_1Mn_8 catalyst and the order of activity of various calcination condition is as follows: Reactive calcination> Flowing air > Stagnant air. Due to the addition of different dopant into the Cu_1Mn_8 catalyst, they have an attribute to the high surface area, amorphous in structure and creation of surface adsorbed oxygen it enhance the mobility of lattice oxygen. The performance of 3%AgCuMn$_8$Ox catalyst is accordance with the results of characterization. The best activity is also exhibited both by their excellent long term stability and good cycling activity due to the presence of their crystalline nature.